Elevated critical temperature at BCS superconductor–band insulator interfaces

Mats Barkman ⬤, Albert Samoilenka ⬤, Andrea Benfenati ⬤, and Egor Babaev
Department of Physics, Royal Institute of Technology, SE-106 91 Stockholm, Sweden

We consider the interface between a Bardeen-Cooper-Schrieffer superconductor and nonsuperconducting band insulator. We show that under certain conditions, such interfaces can have an elevated superconducting critical temperature, without increasing the strength of the pairing interaction at the interface. We identify the regimes where the interface critical temperature exceeds the critical temperature associated with a superconductor-vacuum interface.

I. INTRODUCTION

A series of classical works by de Gennes *et al.* [1–4] considered the interface between a Bardeen-Cooper-Schrieffer (BCS) superconductor and a normal material without electron pairing. The calculations predicted superconducting gap suppression at the interface. The same calculation predicted that in the limit where the material of the interface is dielectric, the normal derivative of the superconducting gap becomes zero. Hence in that limit, superconductivity is neither enhanced nor suppressed near such an interface (similar results were obatined in [5,6]). The zero normal derivative of the superconducting gap is widely considered to be independent of the specifics of the dielectric involving *s*-wave superconductors unless the superconductor is anisotropic (for a review see [6]). In the anisotropic case the superconducting gap can be suppressed near the dielectric interface [6,7].

The problem of the boundary between a superconductor and vacuum was recently revisited. It was shown in [8–10] that there are boundary states in a BCS superconductor that have higher critical temperature than the critical temperature of the bulk. A rigorous mathematical proof of that result was recently presented in [11]. These are highly inhomogeneous solutions for the superconducting order parameter $\Delta(\mathbf{r})$, localized on a macroscopic lengths scale near the surface. The origin of the effect is rooted in interference effects (that were neglected in [1–5]) arising when electrons scatter from a perfectly reflecting surface. The effect requires the solution of the full microscopic model and is not captured in a straightforward application of quasiclassical approximation or Ginzburg-Landau model. However, effective models can capture these states with appropriate microscopically derived boundary conditions [10]. There are various degrees of ex-

perimental evidence of enhanced surface superconductivity in various superconductors [12–22].

In this work we revisit the problem of the interface between a superconductor and normal material. We show that interfaces between BCS superconductors and band insulators, depending on the nature of the dielectric, can have elevated critical temperatures, without the introduction of a new boundary pairing mediator (the effect of additional pairing mediators at interfaces was considered in [23]). The critical temperature of such an interface can even exceed the critical temperature of the perfectly reflective superconductor-vacuum boundary [8–10].

II. MODEL

We model the superconducting-normal interfaces using a mean-field microscopic lattice model, described by the Hamiltonian

$$H = - \sum_{\sigma, \langle xx' \rangle} t(x, x') c_\sigma^\dagger(x) c_\sigma(x') - \sum_{\sigma, x} \mu(x) c_\sigma^\dagger(x) c_\sigma(x)$$
$$+ \sum_x (\Delta(x) c_\uparrow^\dagger(x) c_\downarrow^\dagger(x) + \text{H.c.}), \quad (1)$$

where $c_\sigma(x)$ is the annihilation operator of an electron with spin σ at position x, $\langle xx' \rangle$ denotes nearest-neighbor pairs, and H.c. denotes Hermitian conjugation. The hopping parameters $t(x, x')$ and the on-site chemical potentials $\mu(x)$ are not necessarily the same in both materials. The hopping parameter can take three values: t_S in the superconductor, t_{int} at the interface, and t_N in the nonsuperconducting material. Analogously, the on-site chemical potential can either be equal to μ_S or μ_N. This is illustrated in Fig. 1. The superconducting pairing amplitude $\Delta(x)$ is defined through the thermal average

$$\Delta(x) = V(x) \langle c_\uparrow(x) c_\downarrow(x) \rangle, \quad (2)$$

where $V(x)$ is the pairing potential which equals zero in the normal material. In this paper we are interested in computing the critical temperature of the interface. For a phase transition where $\Delta(x)$ vanishes continuously at criticality, the standard approach is to use a linearized gap equation to find the critical
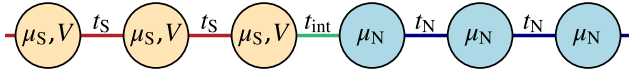
FIG. 1. Illustration of the lattice model for the superconductor-normal interface. The superconductor (to the left) has nonzero pairing potential V, on-site potential μ_S, and hopping parameter t_S. Similarly the normal material (to the right) has some on-site potential μ_N and hopping parameter t_N, but no pairing interaction. The two materials are linked through a hopping parameter t_{int}.

temperature. The linearized gap equation reads

$$\Delta(x) = V(x) \sum_{x'} K(x, x') \Delta(x'), \tag{3}$$

where $K(x, x')$ can be expressed in terms of the wave functions $\phi_{\sigma n}(x)$ in the absence of superconductivity and their corresponding eigenvalues $\epsilon_{\sigma n}$ as

$$K(x, x') = \sum_{m,n} F_{mn} \phi_{\uparrow m}(x) \phi_{\downarrow n}(x) \phi_{\uparrow m}^*(x') \phi_{\downarrow n}^*(x'), \tag{4}$$

and

$$F_{mn} = \frac{1 - f(\beta \epsilon_{\uparrow m}) - f(\beta \epsilon_{\downarrow n})}{\epsilon_{\uparrow m} + \epsilon_{\downarrow n}}, \tag{5}$$

where $f(z) = [1 + \exp(z)]^{-1}$ is the Fermi-Dirac distribution function and $\beta = (k_B T)^{-1}$ is the inverse temperature. At the critical temperature T_c, the largest eigenvalue to the matrix $V(x)K(x, x')$ equals 1. We determine the wave functions and their corresponding eigenvalues numerically, from which the matrix $K(x, x')$ can be constructed and the critical temperature computed.

III. RESULTS

Let us study the influence on the interface critical temperature from the on-site potential μ_N in the nonsuperconducting material. We measure all energies in units of the hopping parameter t_S in the superconductor and therefore set $t_S = 1$. For simplicity, let us assume that all other hopping parameters $t_{int} = t_N = 1$. This leaves us with three variables: the pairing potential V and the two on-site potentials μ_S and μ_N. We consider coupling strength $V = 2$, for which bulk superconductivity is present for $|\mu_S| \lesssim 2.2357$. For values outside this range, both the bulk critical temperature T_{c1} and the hard-wall boundary critical temperature T_{c2} (corresponding to $t_{int} = 0$) vanish. Note also that the boundary critical temperature T_{c2} is larger than the bulk critical temperature T_{c1} only for $|\mu_S| \lesssim 1.7284$. We compute the critical temperature of the superconductor-normal interface for various values of the on-site potential μ_N in the normal material. The resulting critical temperatures are shown in Fig. 2. Note that $T_c(\mu_S, \mu_N) = T_c(-\mu_S, -\mu_N)$, which is a consequence of particle-hole symmetry. At half-filling in the superconductor, that is, $\mu_S = 0$ ($\langle n_\uparrow + n_\downarrow \rangle = 1$), increasing the magnitude of the on-site potential has the effect of increasing the interface critical temperature T_c from T_{c1} at $\mu_N = 0$, to T_{c2} as $\mu_N \to \infty$. For nonzero on-site potential in the superconductor, beyond half-filling, the situation is different. We notice that the interface critical temperature can exceed the hard-wall critical
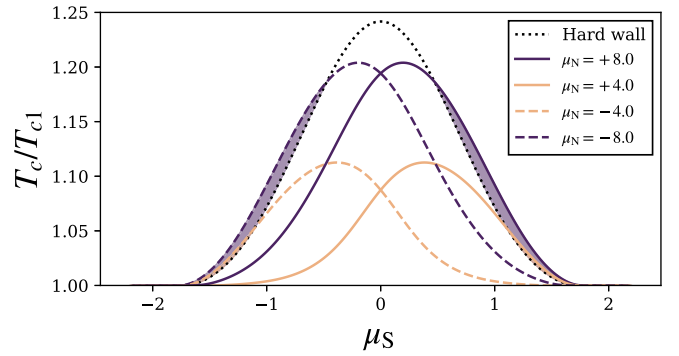

FIG. 2. Interface critical temperature T_c in units of the bulk critical temperature T_{c1} for some fixed on-site potentials μ_N in the normal material, as a function of the on-site potential μ_S in the superconductor. The dotted line corresponds to the hard-wall boundary critical temperature T_{c2}. It shows that it is possible that the interface between a superconductor and band insulator can have higher critical temperature than a superconductor-vacuum interface. All hopping parameters $t_S = t_N = t_{int} = 1$ and superconducting pairing potential $V = 2$.

temperature T_{c2} for some values of the on-site potential μ_N. For positive values of μ_S, this occurs when μ_N also is positive. We show for which parameters the interface critical temperature exceeds the hard-wall critical temperature in Fig. 3. We notice five different parameter regimes. For low magnitudes of the normal on-site potential μ_N, the interface critical temperature does not exceed the bulk critical temperature (region I). As the magnitude of μ_N increases, so does the interface critical temperature. The interface critical temperature exceeds the bulk critical temperature in region II and increases beyond the hard-wall critical temperature in region III. As the magnitude of μ_N approaches infinity, the interface critical approaches the hard-wall critical temperature from above in region III and from below in region II. Region IV corresponds to the
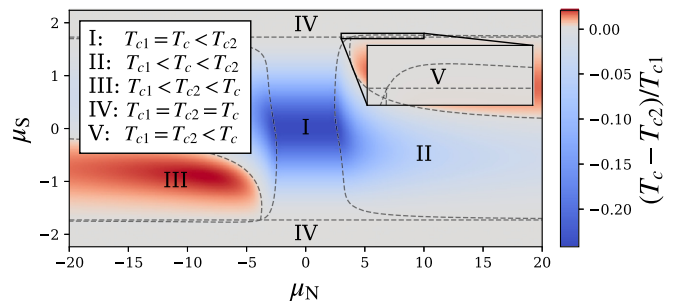

FIG. 3. Difference between the superconductor-normal interface critical temperature T_c and the critical temperature of superconductor-vacuum interface T_{c2} (in units of bulk critical temperature T_{c1}) for various on-site potentials μ_S and μ_N in the superconductor and the normal material, respectively. The blue (red) parameter regime shows where the interface critical temperature is lower (higher) than the critical temperature of a superconductor-vaccuum boundary. The plane is partitioned into five regions, based on the relation between the interface, hard-wall, and bulk critical temperatures (T_c, T_{c2}, and T_{c1}, respectively). All hopping parameters $t_S = t_N = t_{int} = 1$ and superconducting pairing potential $V = 2$.

parameters where all the three critical temperatures are equal. There also exists a fifth region where the hard-wall and bulk critical temperatures are equal and slightly smaller than the interface critical temperature. This regime is very narrow for this particular case. To summarize, we find that the interface between a BCS superconductor and a normal material can have a critical temperature that exceeds the bulk critical temperature, even without additional pairing mediators at the interface. For the considered model, it is necessary that $|\mu_N| \gtrsim 2.45$, which equates to the condition that the non-superconducting material is insulating (since $|\mu/t| > 2$ leads to a completely filled or empty band at zero temperature). The critical temperature of the interface can furthermore be larger than the perfectly reflective superconductor-vacuum boundary, for larger values of $|\mu_N|$. In Appendix A and Fig. 7 we demonstrate enhanced interface critical temperatures for two-dimensional materials. This indicates that the effects shown in the one-dimensional case also are present in higher dimensions.

In the previous example, we studied an interface where we only changed the on-site potentials, keeping all hopping parameters equal. However, the hopping parameter at the interface is, in general, different from the hopping parameters inside the materials. To consider a more general situation, we will now vary the hopping parameter t_{int} at the interface, along with the on-site potentials, keeping the hopping parameters in the superconductor and the normal material $t_S = t_N = 1$ fixed. Let us restrict ourselves to positive on-site potentials. In the case when all hopping parameters are equal, as in Fig. 3, we do observe enhanced interface critical temperatures, however, only for on-site potentials μ_S in the superconductor for which there is also superconductivity in the bulk (for $|\mu_S| \lesssim 2.2357$). Outside this parameter range, the bulk and hard-wall boundary critical temperatures equal zero. However, if the interface hopping parameter t_{int} differs from the hopping parameter in the superconductor, the interface critical temperature can be nonzero even when the bulk critical temperature is zero. This is shown in Fig. 4, where the interface critical temperature is nonzero for larger values of μ_S. For increasing values of μ_S, the critical temperature decreases and the regime in μ_N with nonzero critical temperatures becomes more narrow. Increasing the interface hopping parameter t_{int} results in enhanced critical temperatures and larger parameter regimes that support interface superconductivity.

Having demonstrated that superconductor-band insulator interfaces support enhanced critical temperatures, the natural next question is by how much the critical temperature of such interfaces can be enhanced (without additional interface pairing mediators). Let us begin with keeping both the hopping parameters in the superconducting and normal materials fixed at $t_S = t_N = 1$. For each on-site potential μ_S in the superconductor, we want to find the normal on-site potential μ_N and the interface hopping t_{int} such that the interface critical temperature is maximal. The maximal interface critical temperature is obtained in the limit where both t_{int} and μ_N are large, while keeping the ratio t_{int}^2/μ_N constant (for details see Appendix B). We can also check that the limiting critical temperature and optimal ratio t_{int}^2/μ_N does in fact not depend on the hopping parameter t_N in the normal material. This holds for all values of the superconducting on-site potential
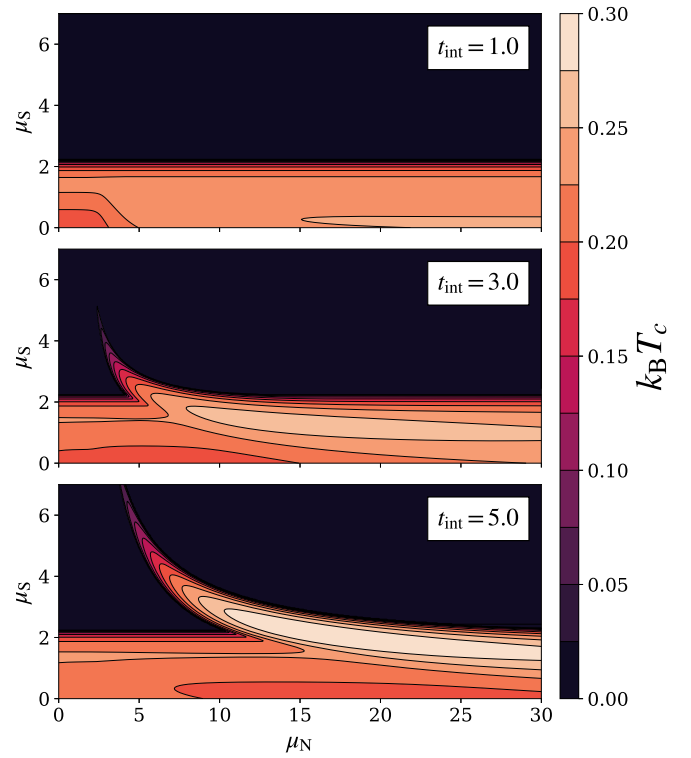

FIG. 4. Interface critical temperature for different values of the interface hopping parameter t_{int}. As t_{int} increases, interface superconductivity can arise in parameter regimes which do not support bulk superconductivity (for $|\mu_S| \gtrsim 2.2357$). Increasing the interface hopping parameter results in larger critical temperatures and wider parameter regimes that support interface superconductivity. Remaining parameters are set to $V = 2$ and $t_S = t_N = 1$.

μ_S, which allows us to compute the maximal interface critical temperature for each μ_S (the optimal ratio t_{int}^2/μ_N does of course also depend on μ_S).

We have shown that to maximize the critical temperature of the interface with a normal material, one should take the limit of large μ_N and t_{int} at a constant ratio t_{int}^2/μ_N. The optimal value of this ratio depends on the on-site potential in the superconductor μ_S, but is independent of the hopping parameter t_N in the normal material. The origin of this result can be understood by analyzing the linear gap equation. The critical temperature is uniquely determined by the superconducting pairing potential $V(x)$ and the wave functions $\phi_{\sigma n}(x)$ and their eigenvalues $\epsilon_{\sigma n}$ in the absence of superconductivity. In the limit where both t_{int} and μ_N are large, only the states that are predominantly localized inside the superconductor give nonnegligible contributions to the linear gap equation. These wave functions decay exponentially inside the normal material on a extremely short lengthscale. Therefore it is sufficient to consider only one site of normal material. Let $x = 0$ be the last superconducting site and $x = 1$ first and only relevant normal site. The Schrödinger equation at site $x = 1$ reads

$$-t_{int}\phi(0) - \mu_N\phi(1) - t_N\phi(2) = \epsilon\phi(1), \qquad (6)$$

where we dropped the indices σ and n for brevity. As stated above, $\phi(2)$ is small and can be neglected. By expressing $\phi(1)$ in terms of $\phi(0)$ and inserting this relation into the equation at
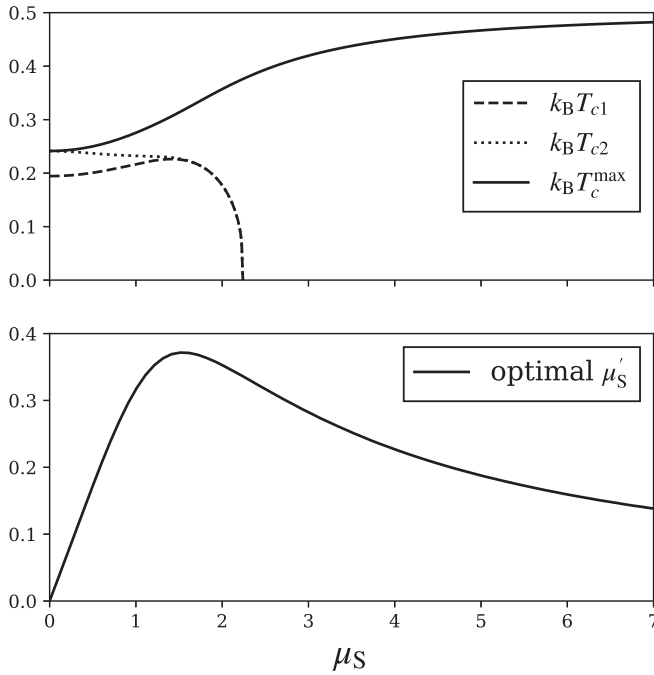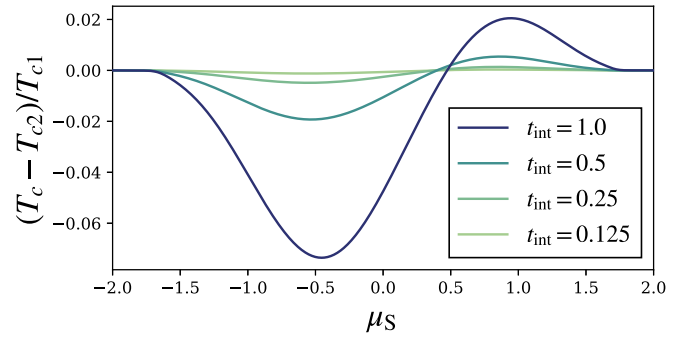
FIG. 6. Difference between interface critical temperature T_c and hard-wall critical temperature T_{c2} (in units of bulk critical temperature T_{c1}), for weakly coupled interfaces (small t_{int}), and for a fixed on-site potential $\mu_N = 8$ in the nonsuperconducting material. This shows that, even for weakly coupled interfaces, there is still a difference between the hard-wall critical temperature and the interface critical temperature, although less pronounced. The hopping parameters $t_S = t_N = 1$ and the superconducting pairing potential $V = 2$.

FIG. 5. Upper panel: Bulk critical temperature T_{c1}, hard-wall critical temperature T_{c2}, and maximal interface critical temperature T_c^{max} for different values of the on-site potential μ_S in the superconductor. Both the bulk and hard-wall critical temperature approach zero simultaneously, while the maximal interface critical temperature increases, approaching its asymptote $V/4$ as μ_S approaches infinity. Lower panel: Optimal shifted on-site chemical potential μ'_S at the interface boundary. As μ_S approaches infinity, μ'_N goes to zero. The superconducting pairing potential $V = 2$ and the hopping parameter $t_S = 1$.

site $x = 0$ gives

$$-t_S\phi(-1) - \left(\mu_S - \frac{t_{int}^2}{\mu_N + \epsilon}\right)\phi(0) = \epsilon\phi(0). \quad (7)$$

The ratio $t_{int}^2/(\mu_N + \epsilon) \simeq t_{int}^2/\mu_N$ in the limit of large μ_N. We can identify Eq. (7) as the equation for hard-wall interface (i.e., superconductor-vacuum boundary), where the on-site potential on the boundary site has been shifted. This shows that, in this particular limit, solving the linear gap equation for the full superconductor-normal interface is equivalent to solving the linear gap equation for a superconductor-vacuum boundary, where the on-site potential on the last superconducting site was shifted to $\mu'_S = \mu_S - t_{int}^2/\mu_N$. We can use this equivalence to easily compute the optimal ratio t_{int}^2/μ_N (or equivalently optimal μ'_S) and the maximal interface critical temperature, for each on-site potential μ_S in the superconductor. This shift in the on-site potential at the boundary changes locally the density of states and will affect the interface critical temperature. The resulting interface critical temperature is shown in Fig. 5, along with the bulk and hard-wall critical temperatures T_{c1} and T_{c2}. At half-filling ($\mu_S = 0$), the maximal interface critical temperature equals the hard-wall critical temperature. As μ_S increases, note that both the bulk and hard-wall critical temperature approaches zero simultaneously, while the interface between these

nonsuperconducting materials remains superconducting and the corresponding critical temperature increases with μ_S. In the limit of large μ_S, it is sufficient to study superconductivity only at the last superconducting site, where the effective on-site potential was shifted. The linear gap equation for this single site becomes

$$1 = V\frac{\tanh\left(\frac{\mu'_S}{2k_BT_c}\right)}{2\mu'_S}, \quad (8)$$

where $\mu'_S = 0$ results in the maximal critical temperature $k_BT_c = V/4$. We can indeed see that this value is approached as $\mu_S \to \infty$ in Fig. 5 (where $V = 2$).

We showed that, to additionally enhance the interface critical temperature, the interface hopping parameter t_{int} should be large. For completeness case, let us also study the limit of small t_{int}, that is weakly coupled superconductor-normal interfaces. We know that when $t_{int} = 0$, the interface critical temperature equals the hard-wall critical temperature T_{c2}. We show the difference between the interface and hard-wall critical temperatures in Fig. 6 for $t_{int} \leqslant 1$, and for $\mu_N = 8$. We see that even for small t_{int}, the two critical temperatures differ and the interface critical temperature can exceed the hard-wall critical temperature. As expected, the difference approaches zero as $t_{int} \to 0$.

IV. CONCLUSION

In conclusion, we revisited the problem of a boundary between a BCS superconductor and a nonsuperconducting material. We showed that when the nonsuperconducting material is a band insulator the interface can acquire an elevated superconducting critical temperature. The effect arises in basic BCS theory (i.e., without the introduction of a new interface pairing mediator) and is closely connected with the
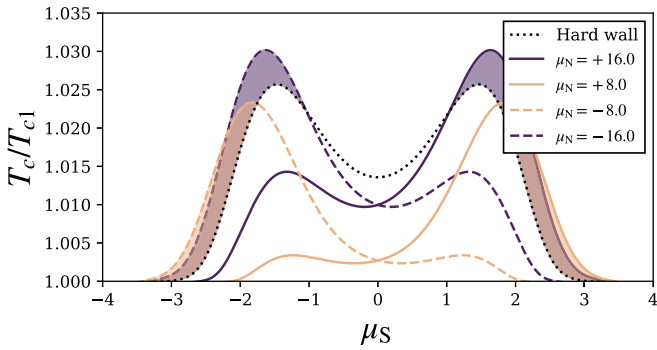
FIG. 7. Example of enhanced interface critical temperature T_c (in units of bulk critical temperature T_{c1}) for a two-dimensional square lattice. Similarly as in the one-dimensional case in Fig. 2, beyond half-filling there exists regimes where the interface critical temperature can exceed the hard-wall critical temperature. The hopping parameters $t_S = t_N = t_{int} = 1$ and the superconducting pairing potential $V = 3$.

nature of electronic scattering from the interface. The critical temperature of a superconductor-band insulator interface is in general different from, and can exceed, the elevated critical temperature associated with a perfectly reflective superconductor-vacuum boundary [8–10]. This suggests investigating granular materials with well-insulating oxides and superconductor-insulator metamaterials as a possible route to engineer improved superconducting properties.

ACKNOWLEDGMENT

APPENDIX A: EXAMPLE IN THE TWO-DIMENSIONAL CASE

Here we show that the enhancement of interface critical temperature does not only occur in the simplest one-dimensional case (studied in the main text), but is also present in the two-dimensional case. Similarly as in Fig. 2, we study the interface critical temperature for the two-dimensional interface in Fig. 7 for different chemical potentials in the superconductor and the normal material. We find that the interface critical temperature can exceed both the bulk critical temperature T_{c1} and the hard-wall critical temperature T_{c2}.

APPENDIX B: EXTRAPOLATING MAXIMAL CRITICAL TEMPERATURE

We want to determine the largest possible interface critical temperature for each on-site potential μ_S in the superconductor. To be specific, we want to maximize the critical
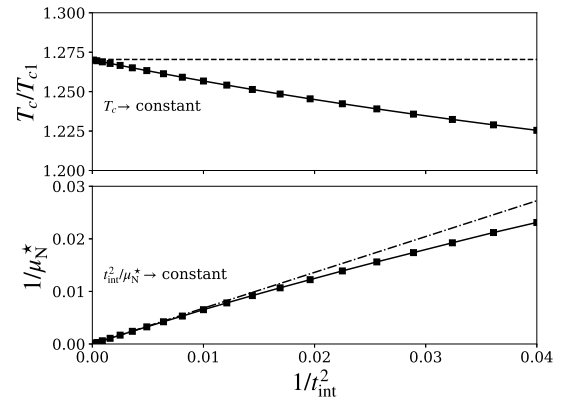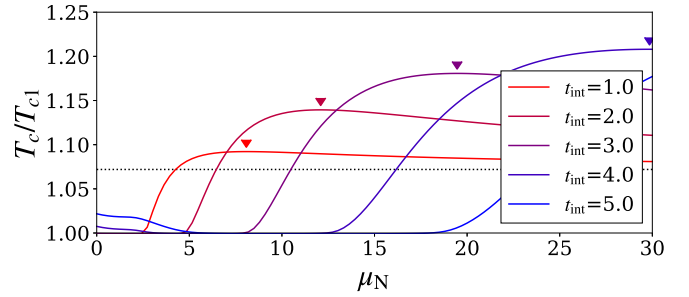

FIG. 8. Upper panel: Interface critical temperature T_c as a function of the normal on-site potential μ_N for various interface hopping parameters t_{int}. The triangles mark the optimal on-site potential $\mu_N^\star$ where the critical temperature is maximal. Both the optimal on-site potential $\mu_N^\star$ and the associated critical temperature increases as t_{int} increases. For comparison, the dotted line corresponds to the hard-wall critical temperature T_{c2}. Middle and lower panel: Maximal critical temperature and optimal on-site potential for large t_{int}. The critical temperature approaches its upper bound (indicated by dashed line), while $\mu_N^\star$ diverges as t_{int}^2 (see the dash-dotted line). Remaining parameters are set to $V = 2$, $t_S = t_N = 1$, and $\mu_S = 1$.

temperature with respect to the remaining parameters: t_{int} and μ_N (for simplicity we begin with fixing the hopping parameter in the normal material $t_N = 1$). For each considered t_{int}, we span over μ_N to find the maximal critical temperature. An example of such spans is shown in Fig. 8, where $\mu_S = 1$. For each interface hopping t_{int}, we locate the on-site potential $\mu_N^\star$ that maximizes the critical temperature. We observe that as t_{int} increases, so does $\mu_N^\star$, along with the corresponding critical temperature. To find an upper bound on the possible interface critical temperature in this model, we can extrapolate the behavior for very large t_{int}, also shown in Fig. 8 for this particular value of μ_S. We see that the critical temperature approaches some constant for large t_{int}, while the optimal on-site potential $\mu_N^\star$ scales as t_{int}^2. The limiting critical temperature and the optimal ratio $t_{int}^2/\mu_N^\star$ are independent of the hopping parameter t_N in the normal material.

[1] P. G. De Gennes, *Superconductivity of Metals and Alloys*, Advanced Book Classics (CRC Press, Boca Raton, FL, 1999).

[2] P. G. De Gennes, Boundary effects in superconductors, Rev. Mod. Phys. **36**, 225 (1964).

[3] C. Caroli, P. G. De Gennes, and J. Matricon, Coherence length and penetration depth of dirty superconductors, Phys. Kondens. Mater. **1**, 176 (1963).

[4] C. Caroli, P. G. De Gennes, and J. Matricon, Sur certaines propriétés des alliages supraconducteurs non magnétiques, J. Phys. Radium **23**, 707 (1962).

[5] A. A. Abrikosov, Concerning surface superconductivity in strong magnetic fields, Sov. Phys. JETP **20**, 480 (1965).

[6] E. A Andryushin, V. L. Ginzburg, and A. P. Silin, Boundary conditions in the macroscopic theory of superconductivity, Phys. Usp. **36**, 854 (1993).

[7] E. A. Shapoval, Boundary conditions on the ginzburg-landau equations for anisotropic superconductors, Zh. Eksp. Teor. Fiz. **88**, 1073 (1985).

[8] A. Samoilenka and E. Babaev, Boundary states with elevated critical temperatures in bardeen-cooper-schrieffer superconductors, Phys. Rev. B **101**, 134512 (2020).

[9] A. Samoilenka, M. Barkman, A. Benfenati, and E. Babaev, Pair-density-wave superconductivity of faces, edges, and vertices in systems with imbalanced fermions, Phys. Rev. B **101**, 054506 (2020).

[10] A. Samoilenka and E. Babaev, Microscopic derivation of superconductor-insulator boundary conditions for ginzburg-landau theory revisited: Enhanced superconductivity at boundaries with and without magnetic field, Phys. Rev. B **103**, 224516 (2021).

[11] C. Hainzl, B. Roos, and R. Seiringer, Boundary superconductivity in the bcs model, arXiv:2201.08090.

[12] H. J. Fink and W. C. H. Joiner, Surface Nucleation and Boundary Conditions in Superconductors, Phys. Rev. Lett. **23**, 120 (1969).

[13] R. Lortz, T. Tomita, Y. Wang, A. Junod, J. S. Schilling, T. Masui, and S. Tajima, On the origin of the double superconducting transition in overdoped YBa$_2$Cu$_3$O$_x$, Physica C: Superconductivity **434**, 194 (2006).

[14] E. Janod, A. Junod, T. Graf, K.-Q. Wang, G. Triscone, and J. Muller, Split superconducting transitions in the specific heat and magnetic susceptibility of YBa$_2$Cu$_3$O$_x$ versus oxygen content, Physica C: Superconductivity **216**, 129 (1993).

[15] I. N. Khlyustikov, Critical magnetic field of surface superconductivity in lead, J. Exp. Theor. Phys. **113**, 1032 (2011).

[16] I. N. Khlyustikov, Surface superconductivity in lead, J. Exp. Theor. Phys. **122**, 328 (2016).

[17] V. F. Kozhevnikov, M. J. V. Bael, P. K. Sahoo, K. Temst, C. V. Haesendonck, A. Vantomme, and J. O. Indekeu, Observation of wetting-like phase transitions in a surface-enhanced type-i superconductor, New J. Phys. **9**, 75 (2007).

[18] I. N. Khlyustikov, Surface Superconductivity of Vanadium, J. Exp. Theor. Phys. **132**, 453 (2021).

[19] I. Mangel, I. Kapon, N. Blau, K. Golubkov, N. Gavish, and A. Keren, Stiffnessometer: A magnetic-field-free superconducting stiffness meter and its application, Phys. Rev. B **102**, 024502 (2020).

[20] M. I. Tsindlekht, G. I. Leviev, I. Asulin, A. Sharoni, O. Millo, I. Felner, Yu. B. Paderno, V. B. Filippov, and M. A. Belogolovskii, Tunneling and magnetic characteristics of superconducting ZrB$_{12}$ single crystals, Phys. Rev. B **69**, 212508 (2004).

[21] M. Belogolovskii, I. Felner, and V. Shaternik, Zirconium dodecaboride, a novel superconducting material with enhanced surface characteristics, in *Boron Rich Solids*, edited by N. Orlovskaya and M. Lugovy (Springer Netherlands, Dordrecht, The Netherlands, 2011), pp. 195–206.

[22] R. Khasanov, D. Di Castro, M. Belogolovskii, Yu. Paderno, V. Filippov, R. Brütsch, and H. Keller, Anomalous electron-phonon coupling probed on the surface of superconductor ZrB$_{12}$, Phys. Rev. B **72**, 224509 (2005).

[23] V. L. Ginzburg, On surface superconductivity, Phys. Lett. **13**, 101 (1964).